Journal of Research and Applications in Mechanical Engineering
ISSN: 2229-2152 (Print); 2697-424x (Online)
(2021) Vol. 9, No. 1, Paper No. JRAME-21-9-003
[DOI: 10.14456/jrame.2021.3]

Research Article

MODELLING AND CONTROL OF AN UNDERWATER GLIDER

P. Jantapremjit[1,*]
K. Daengchart[1]
P.A. Wilson[2]
[1]Department of Mechanical Engineering, Faculty of Engineering, Burapha University Mueng, Chonburi 20131, Thailand
[2]Faculty of Engineering and Physical Sciences, University of Southampton, Southampton SO16 7QF, UK

Received 22 July 2020
Revised 22 September 2020
Accepted 27 September 2020

ABSTRACT:
Generally, underwater gliders are used for various underwater explorations. Their advantages are low energy consumption and long-range application. This paper describes a modelling and control design of an underwater glider. The nonlinear dynamic model is complexed, thus the simplified mathematical model of an underwater glider is obtained. System identification of the vehicle is investigated. The work presents the depth and pitch angle control design using PID and LQR controllers. The computer simulation and experiment results are compared for the performance of the proposed control schemes.

Keywords: *Underwater glider, PID control, LQR control*

1. INTRODUCTION

Underwater vehicles are widely utilised in remote sensing applications for oceanography [1], for example, marine life exploration, surveillance and monitoring, undersea geography information and military mission [2]. Underwater vehicles are conventionally divided two types, namely, manned underwater vehicles and unmanned underwater vehicles. The unmanned vehicles are either autonomous underwater vehicles (AUVs) or remotely operated underwater vehicles (ROVs). A recent development of unmanned platform are underwater gliders [3]. Their capability of an extra-long range operation with minimised energy consumption without manned control is the main challenge of this vehicle. They can autonomously operate both individual or in group. The idea of underwater gliders was inspired by [4] and has been continually developed for decades. They have no active thrusters and have some limited external motion control surfaces (rudder). Gliders have external fixed wings and tails. They use buoyancy force and internal mass distribution for moving upward and downward in the ocean. The glider with a buoyancy driven engine is quiet and uses minimum power. Various underwater gliders (see Fig. 1) have been developed and tested for sea trails, for example, Slocum glider [5], Spray glider [6] and Seaglider [7]. Originally, the Slocum is 3.2 m long and 40 kg displacement. Slocum glider uses thermal powered engine, which was able to operate for up to 150 m depth and glide angles from 10° to 40° with longitudinal speed of 0.15 to 0.22 m/s. They aimed to operate in fleets in a coordinate networks (e.g. monitoring grid, feature tracking, station keeping). Spray is 2 m long and 50 kg displacement. Spray glider has a slender ellipsoid shape. This hull shape is a key in design for performance. Spray uses electrical power. It had been successfully tested up to 1,500 m depth with operating speed of 0.2 to 0.3 m/s. Seaglider is 1.8 m long and 52 kg displacement. The vehicle has a low drag axisymmetric shape. It uses battery powered which is able to operate up to 1500 m depth with travelling speed of 0.25 m/s. Apart from pioneer works, there are remarkable glider designs being developed. Those vehicles are ALBAC [8], SeaExplorer glider [9], Rogue [10], Sterne sea glider [11] and USM underwater glider [12].

* Corresponding author: P. Jantapremjit
E-mail address: pakpong@eng.buu.ac.th

(a) (b)

Fig. 1. Underwater gliders: (a) Slocum glider [5] (b) Spray glider [6].

A mathematical model of an underwater glider is required for predicting the system's behaviour. Therefore, it is achieved by deriving the equations of motion of the vehicle's dynamics. There are various works discussed on marine vehicles (see [13-15]). Newtonian and Lagrangian method are used to derive a six degree of freedom of a marine vessel. Underwater glider model was presented in [15]. The model includes buoyancy control, wings and external control and internal mass actuator. It found complication to directly derive a model from the system. Mathematical model of a system can be generated from the first principle [13] and the system identification [16]. System identification method estimates a system characteristics based on input and output data [17]. The data will provide the construction of an empirical mode. Reliable control system for estimating the dynamic models should be investigated to realise the functionality of the underwater glider.

As mentioned earlier, an underwater glider's motion control is very important as it allows a vehicle glides along a predefined path. Feedback control is commonly used in designing controller for a glider's movement. Most of them use the classical controllers such as PID (proportion-integral-derivative) [18-20] and LQR (linear quadratic regulator) [10, 15, 21]. The performance of PID control is acceptable both through theoretical research and long-term practice in the modern control. PID is based on a linear control law whist the underwater glider dynamics are nonlinear [22]. Thus the PID is unable to compensate for unmodelled hydrodynamics and external disturbances. However, advanced control schemes, for example, sliding mode control (SMC) [23-25], neural network control (NN) [26, 27], fuzzy logic control (FLC) [28-30] and model predictive control (MPC) [31] have been extensively developed in the community. SMC is a robust controller design with external disturbance rejection. However chattering [32] is undesirable phenomena of oscillation having finite frequency and amplitude [33]. Multivariable self-tuning and position control using LQR technique has been implemented in [34]. PID with fuzzy controller discussed and investigated in [35]. Neural network control strategy was proposed in [26]. It can handle the nonlinearity and easily adapts to the changing of underwater glider dynamics. A summary of recent control methods for underwater gliders is covered in Table 1.

Table 1: Various control strategies for underwater gliders

Control strategy	Features	Remarks
PID [18-20]	Vertical and lateral motions	Good performance (properly tuned gain), simple control schemes for certain model, not robust to disturbances
LQR [10, 15, 21]	Lateral motion	Feasible optimal control for linear system, proper model for weighting parameters
SMC [23-25]	Lateral motion	Effective and robustness to parameter variation and disturbances, chattering effect
FLC [28-30]	Vertical and lateral motion	Simplified dynamics model, approximation accuracy, good robustness with simple fuzzy process
NN [26, 27]	Lateral motion	Improved robust to parameter uncertainty
MPC [31]	Path following	Prediction capability, robustness, high computational time

In summary, this paper aims to presents preliminary work of the controller design using PID and LQR schemes for the depth and pitch angle control which is applied to an underwater glider. Section 2 presents the underwater glider's kinematics and its simplified dynamics model in the vertical plane. Section 3 presents the system identification for the ballast system and its PID and LQR controller. Section 4 shows the results. Conclusion is given in the last section.

2. MODELLING OF AN UNDERWATER GLIDER

2.1 Kinematics and dynamics

In general, kinematics and dynamics model of an underwater glider are similar to the 6-DOFs nonlinear equation of an underwater vehicle. The notation used in this work defined by SNAME [14]. They are obtained by using a global reference of the NED-frame (North-East-Down) and the body-fixed frame (see Fig. 2).

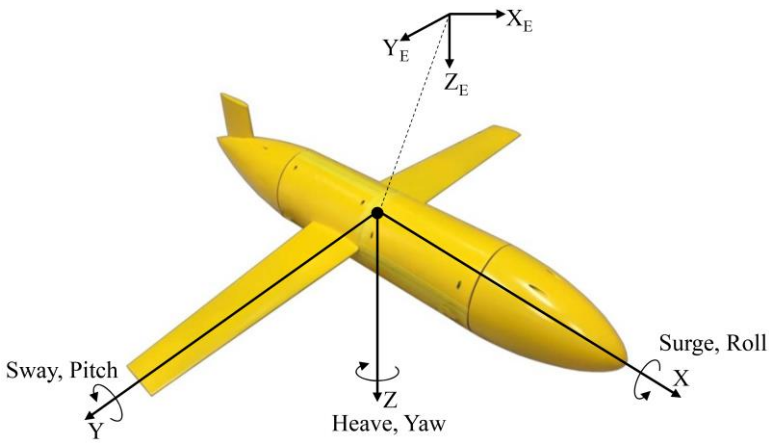

Fig. 2. Frame coordinates of an underwater glider

The kinematic model of an underwater glider in the body-fixed frame is defined as

$$\dot{\eta} = J(\eta)\nu \tag{1}$$

where η is the position and orientation vector decomposed om the earth-fixed frame, $J(\eta)$ is the Jacobian matrix and ν is the linear and angular velocity vector in the body-fixed frame. The rotation and transformation matrix of the Euler angle is therefore obtained by

$$J(\eta) = \begin{bmatrix} R_b^n(\eta) & 0_{3\times3} \\ 0_{3\times3} & T_b^n(\eta) \end{bmatrix} \tag{2}$$

where $R_b^n(\eta)$ and $T_b^n(\eta)$ are the linear and angular velocity transformation, respectively. The dynamics model of an underwater glider is derived from the Newton-Euler equation

$$M\dot{\nu} + C(\nu)\nu + D(\nu)\nu + g(\eta) = \tau \tag{3}$$

where M is the inertia matrix, $C(\nu)$ is the Coriolis and centripetal matrix, $D(\nu)$ is the hydrodynamic damping and lift matrix, $g(\eta)$ is the gravitational and buoyancy forces and moment matrix and τ is the control input vector.

The inertia matrix comprises a rigid body inertia and mass and hydrodynamic added mass which is defined as [36]

$$M = M_{RB} + M_A \tag{4}$$

The Coriolis and centripetal matrix consists of a rigid body Coriolis and centripetal matrix induced from $M_{RB}(\nu)$ and a hydrodynamic added mass which give a Coriolis-like matrix induced from $M_A(\nu)$ which is defined as [36]

$$C(\nu) = C_{RB}(\nu) + C_A(\nu) \tag{5}$$

However, an underwater glider moves by a change of buoyancy. Generally, it uses a separate control methodology and actuators in controlling lateral and vertical plane motions. The vertical plane motion is controlled using a variable ballast mass and an internal movable mass. The lateral plane motion is stabilised because the vehicle has a fixed rudder which allows a straight motion in a vertical plane. An underwater glider has a distribution hull mass (m_h) with a fixed point mass (m_p)is controlled by a variable ballast actuator (m_b) and an internal movable mass (m_m). Figure 3 shows simplified internal mass configuration. The total body mass (m_t) is given as follows

$$m_t = m_h + m_p + m_b + m_m \tag{6}$$

Thus, the net mass due to fluid displaced in the buoyancy engine is given by $m_0 = m_t - m_f$, where m_f is the mass of displaced fluid in the vehicle.

2.2 Equations of motion

Equation of motion of an underwater vehicle is 6-DOFs nonlinear equation of motion [13, 14]. The mode of an underwater glider is similarly suggested in [15]. From Fig. 3, the vertical motion equation is simplified by neglecting the diagonal and coupling terms and tether dynamics. The body-fixed frame of the glider is fixed with its origin at the centre of buoyancy (CB). It is assumed that added masses are constant. The wings contributes the main lift and drag on the whole body when an angle of attack is low, this is because the glider body is symmetry.

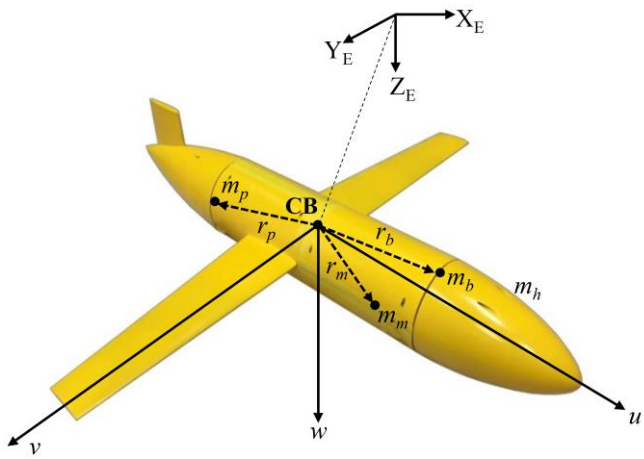

Fig. 3. Simplified internal mass configuration of an underwater glider

The equations of motion in the vertical plane of an underwater glider [22] are given as follows

$$\dot{x} = u\cos\theta + w\sin\theta \tag{7}$$

$$\dot{z} = -u\sin\theta + w\cos\theta \tag{8}$$

$$\dot{\theta} = q \tag{9}$$

where u, w are the translational motion along x, z-axis, respectively, q is the angular velocity and θ is the pitch angle. The angular velocity due to the internal movable mass is now given

$$\dot{q} = \frac{1}{I_y}((m_z - m_x)uw - m_m g(r_{mx}\cos\theta + r_{mz}\sin\theta) + M_{DL} - r_{mz}f_x + r_{mx}f_z) \tag{10}$$

where I_y is the moment of inertia of the rigid-body, m_x, m_z are the element of the system inertia matrix, f_x, f_z are the input force acting on a movable mass and a variable ballast, and M_{DL} is the viscous moment.

The linear velocity of the underwater glider can be rewritten

$$\dot{u} = \frac{1}{m_x}(-m_z wq - p_{mz}q - m_0 g \sin\theta + L \sin\alpha - D\cos\alpha - f_x) \quad (11)$$

$$\dot{w} = \frac{1}{m_z}(m_x uq + p_{mx}q + m_0 g \cos\theta - L \cos\alpha - D\sin\alpha - f_z) \quad (12)$$

where α is the angle attack, D, L are drag force and lift force, respectively. The rate of inertia momentum change gives the equations as shown below

$$\dot{r}_{mx} = \frac{1}{m_m}(\dot{p}_{mx} - u - r_{mz}q) \quad (13)$$

$$\dot{r}_{mz} = \frac{1}{m_m}(\dot{p}_{mz} - w - r_{mx}q) \quad (14)$$

where $\dot{p}_{mx} = f_x$, $\dot{p}_{mz} = f_z$ and $\dot{m}_b = f_b$ is the variable ballast control effort input.

The hydrodynamic forces and moment are expressed as

$$D_f = \frac{1}{2}\rho C_d A_s V^2 \quad (15)$$

$$L_f = \frac{1}{2}\rho C_l A_s V^2 \quad (16)$$

$$M_{DL} = \frac{1}{2}\rho C_m A_s V^2 \quad (17)$$

where D_f, L_f are the drag and lift. M_{DL} is viscous moment. C_d, C_l and C_m are the coefficients of drag, lift and pitch moment, respectively, A_s is the cross section area, ρ is the fluid density and the glider speed $V = \sqrt{u^2 + w^2}$. The parameter values of the underwater glider are shown in Table 2.

Table 2: Parameters of the underwater glider

Parameter	Value	Unit
Length	865	mm
Body diameter	120	mm
Wing length	820	mm
Hull mass	3.2	kg
Variable ballast mass	0.0495	kg
Movable mass	0.324	kg

3. SYSTEM CONTROL DESIGN

3.1 System identification

System identification is an approach for identifying an underwater glider's model. The combination of static and dynamics experiments are implemented with parameters and then estimated using the least squares method. The simplified model is rewritten in the form

$$\lambda = H\Gamma \quad (18)$$

where Γ is a vector of unknown parameters, H is a matrix containing data from the experiment and λ is a vector of known values. The estimation of a parameter is found

$$\Gamma = (H^T H)^{-1} H^T \lambda \quad (19)$$

The standard deviation of the estimated parameter is,

$$\hat{\varphi}_{\Gamma}^{2} = diag(H^{T}H)^{-1}\hat{\varphi}^{2} \tag{20}$$

where $\hat{\varphi}^{2}$ is a variance of the zero-mean Gaussian noise from the data measurement. Within the Bayesian inference, a probability density function λ given $\hat{\varphi}$ is called likelihood function and the estimator expressed in Eq. (18) is named maximum likelihood estimator [37].

The numerical results (see Fig. 4) show each curve fitting from an experimental data of the depth measurement. The cross validation is to ensure the model quality. Percentages of the curve's best fit are 79.83%, 80.18%, 80.78%, 80.27%, respectively. However, a response simulated due to a unit step input and its closed-loop poles are considered. Only linear model #1 (Fig. 4(a)) gives the response rises asymptotically and acts like low pass filter with no finite zeros. Thus it is selected as a candidate structure for constructing a depth transfer function.

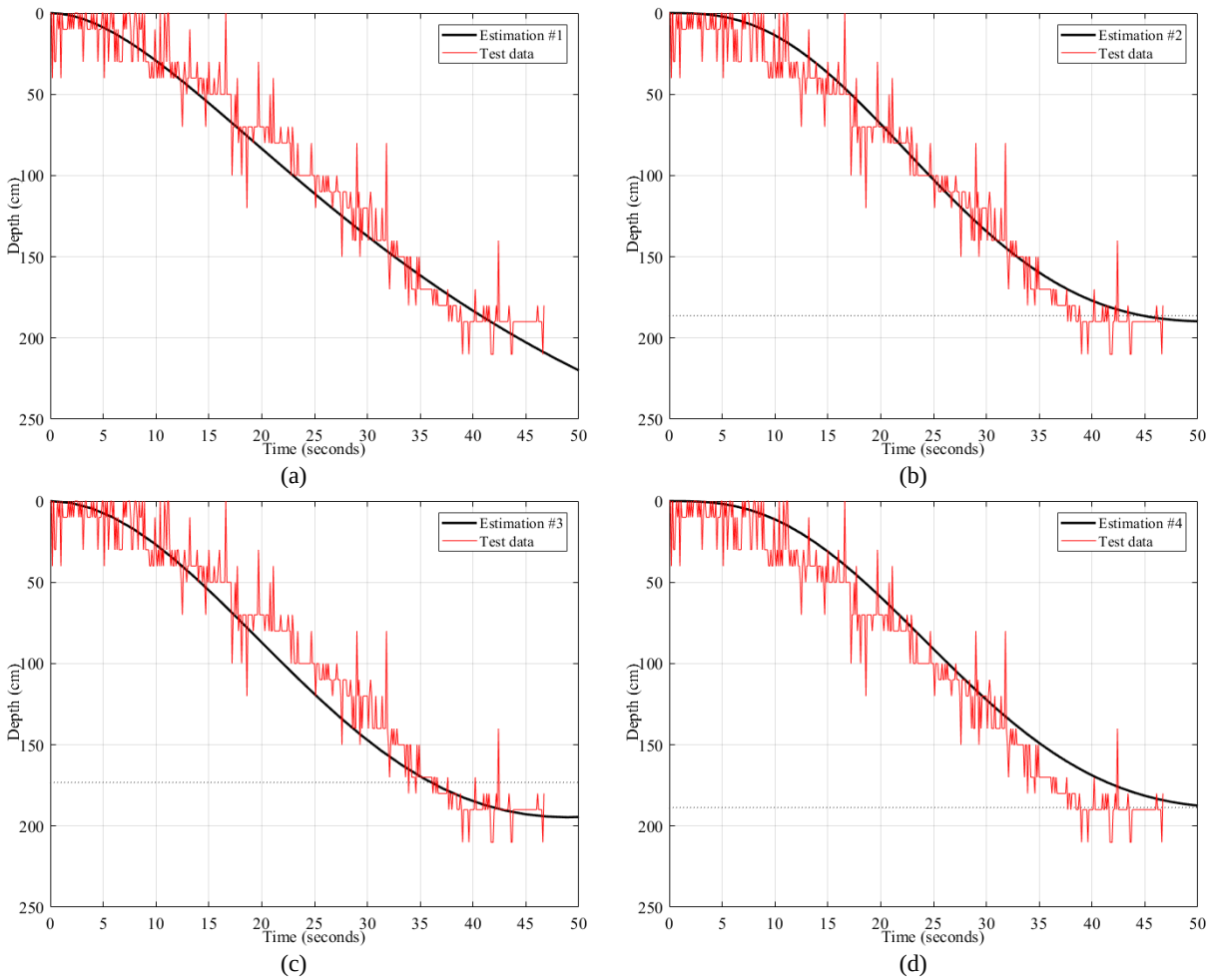

Fig. 4. Depth's curve fitting and it's response with
(a) 79.83% best fit (b) 80.18% best fit (c) 80.78% best fit (d) 80.27% best fit

Figure 5 shows the numerical results of a curve fitting from an experimental data of the pitch angle measurement. The cross validation is to ensure the model quality. Percentages of the curve's best fit are 50.05%, 54.97%, 54.69% and 54.68%, respectively. However, a response simulated due to a unit step input and its closed-loop poles are considered. Only linear model #1 (Fig. 5(a)) gives the response rises asymptotically and acts like low pass filter with no finite zeros. Thus it is selected as a candidate structure for constructing a pitch angle transfer function.

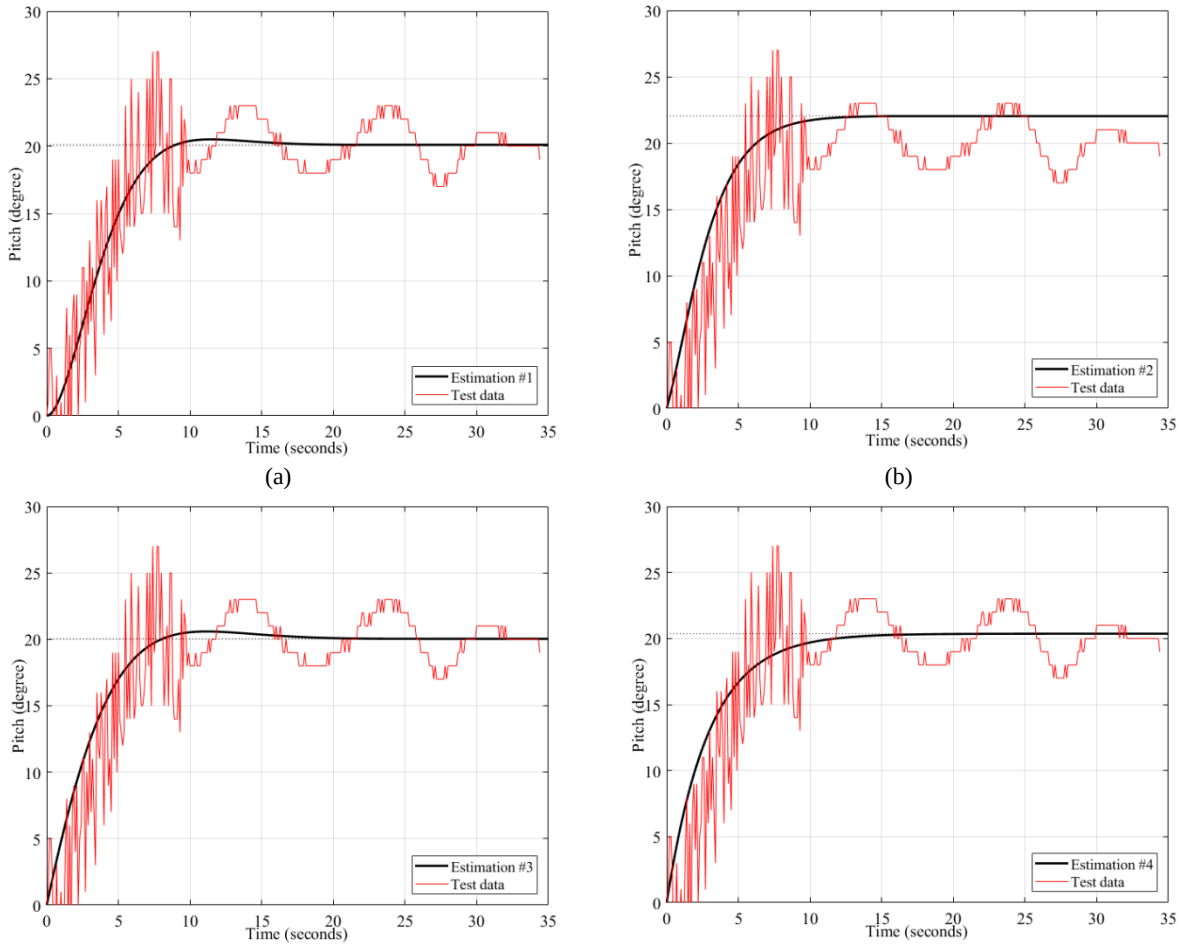

Fig. 5. Pitch's curve fitting and it's response with
(a) 50.05% best fit (b) 54.97% best fit (c) 54.69% best fit (d) 54.68% best fit

3.2 System model

Consider the linear time invariant system in the following equations

$$\dot{x}(t) = Ax(t) + Bu(t)$$
$$y(t) = Cx(t) + Du(t) \tag{21}$$

where $x(t)$ is the state vector, $u(t)$ is the input vector, $y(t)$ is the output vector, A is the state matrix, B is the input matrix, C is the output matrix and D is the feedforward matrix. From system identification, the transfer functions of depth $G_d(s)$ and pitch $G_p(s)$ are found

$$G_d(s) = \frac{2.241}{394.6s^2 + 46.03s + 1} \tag{22}$$

$$G_p(s) = \frac{1.005}{5.207s^2 + 3.564s + 1} \tag{23}$$

The transfer function are now converted into state space forms as follows

$$A_d = \begin{bmatrix} -0.1166 & -0.0025 \\ 1 & 0 \end{bmatrix},\ B_d = \begin{bmatrix} 1 \\ 0 \end{bmatrix},\ C_d = [0 \quad 0.0057],\ D_d = 0 \tag{24}$$

$$A_p = \begin{bmatrix} -0.6837 & -0.192 \\ 1 & 0 \end{bmatrix},\ B_p = \begin{bmatrix} 1 \\ 0 \end{bmatrix},\ C_p = [0 \quad 0.193],\ D_p = 0 \tag{25}$$

3.2.1 PID control

The design of the proportional-integral-derivative (PID) controller is described in this section. It aims to control the pitch angle θ with a constant speed. In the time domain, the PID control law [38] is generally given

$$u(t) = K_P \tilde{e}(t) + K_I \int \tilde{e}(t)dt + K_D \frac{d\tilde{e}(t)}{dt} \tag{26}$$

where K_p, K_I, K_D are proportional, integral and derivative gain. The error signal $\tilde{e}(t) = e_d - e(t)$ measures the difference between the desired input and the actual output. A block diagram of the PID controller design is shown in Fig. 6.

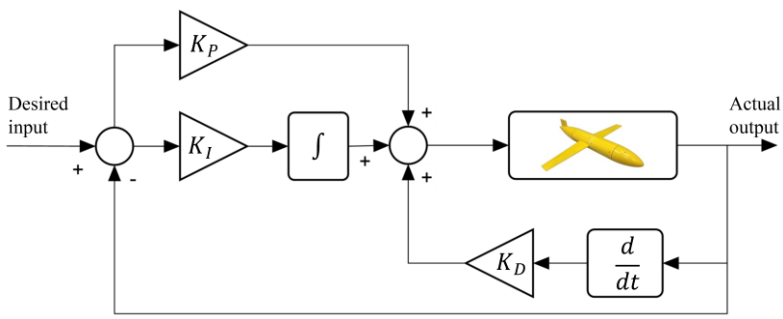

Fig. 6. Block diagram of depth control system using PID controller

Furthermore, a derivative term has a negative gain which is placed in a feedback loop. This is to reduce the kicking phenomenon [38], that usually occurs when there is a sudden change in the desired input. However, the PID control may affect by an integral windup when used in a system in which actuator saturation occurs. A condition of anti-windup in a system is used to overcome significant overshoots. The system performances are then evaluated in term of the overshoot $\%OS$, settling time T_s and steady state error $e(\infty)$.

3.2.2 LQR control

Linear quadratic regulator (LQR) is one of the optimal control methods [39]. The block diagram of LQR controller design is shown Fig. 7. The performance index J is expressed as,

$$J = \int_0^\infty (x(t)^T Q x(t) + u(t)^T R u(t))dt \tag{27}$$

where $Q \geq 0$ and $R > 0$ are symmetric semi-positive definite state and positive control weighting matrix, respectively. Therefor the stability is guaranteed. Selection of the matrix $Q = diag(\epsilon, 0)$ and $R = 1$ is given. The following algebraic Riccati equation can be solved

$$PA + A^T P - PBR^{-1}B^T P + Q = 0 \tag{28}$$

The positive semi-definite matrix P is obtained by solving the above equation. The state feedback gain matrix is

$$K_{LQR} = R^{-1}B^T P \tag{29}$$

The state feedback control law is,

$$u(t) = -K_{LQR}x(t) \tag{30}$$

Thus computing the eigenvalue of $(A - BK)$ where the stable closed-loop poles have negative real part.

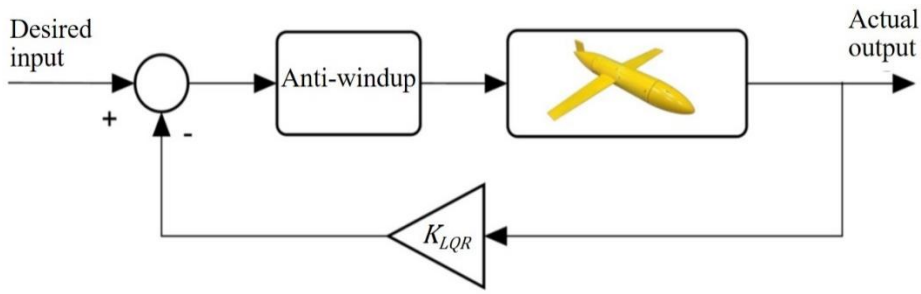

Fig. 7. Block diagram of depth control system using LQR controller

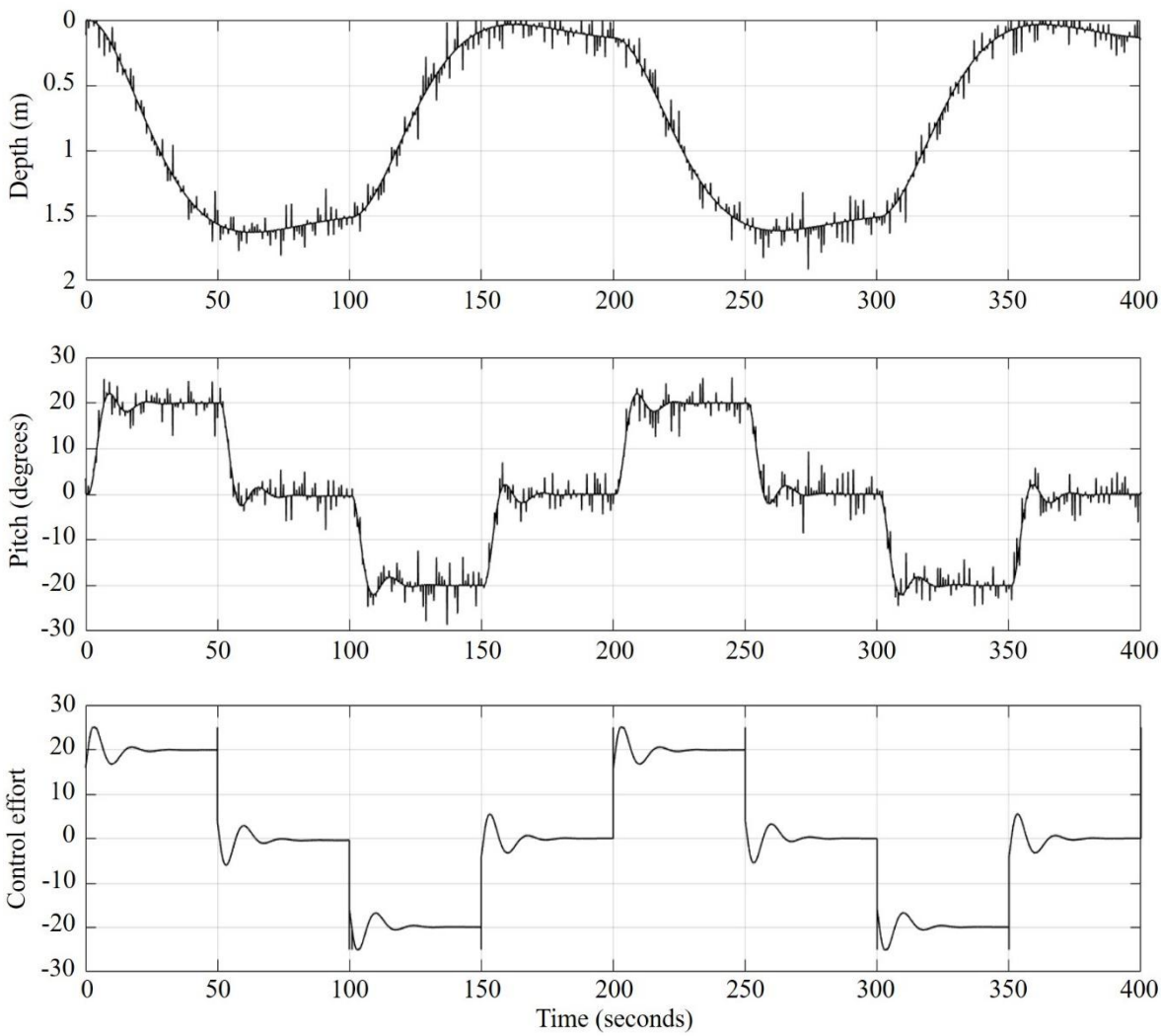

Fig. 8. Results show control performance using PID controller design

4. RESULTS

The PID and LQR controller designs are simulated and performed within a simulation scenario and experiment. The depth controller was implemented by the internal ballast-movable mass actuator. The depth set-point is 1.5 meters to reach each equilibrium downward and upward gliders. A reference depth was measured from the water pressure with 0.5%-1.0% accuracy. The pitch controller was active to maintain a constant pitch angle at ± 20° during gliding maneuvers. A reference pitch angle was obtained from the MPU6050 IMU. However, the underwater glider exhibit rich dynamics, such as waves, unsteady pitching and rolling. The objectives are to examine the performance of both controller designs in term of overshoot, settling time and the steady state error. The results are shown in Fig. 8 and 9. These shown results in the underwater glider reaching a steady glider equilibrium corresponding to the setting. They indicate that the PID and LQR can provide good performance even some disturbances are introduced to the system.

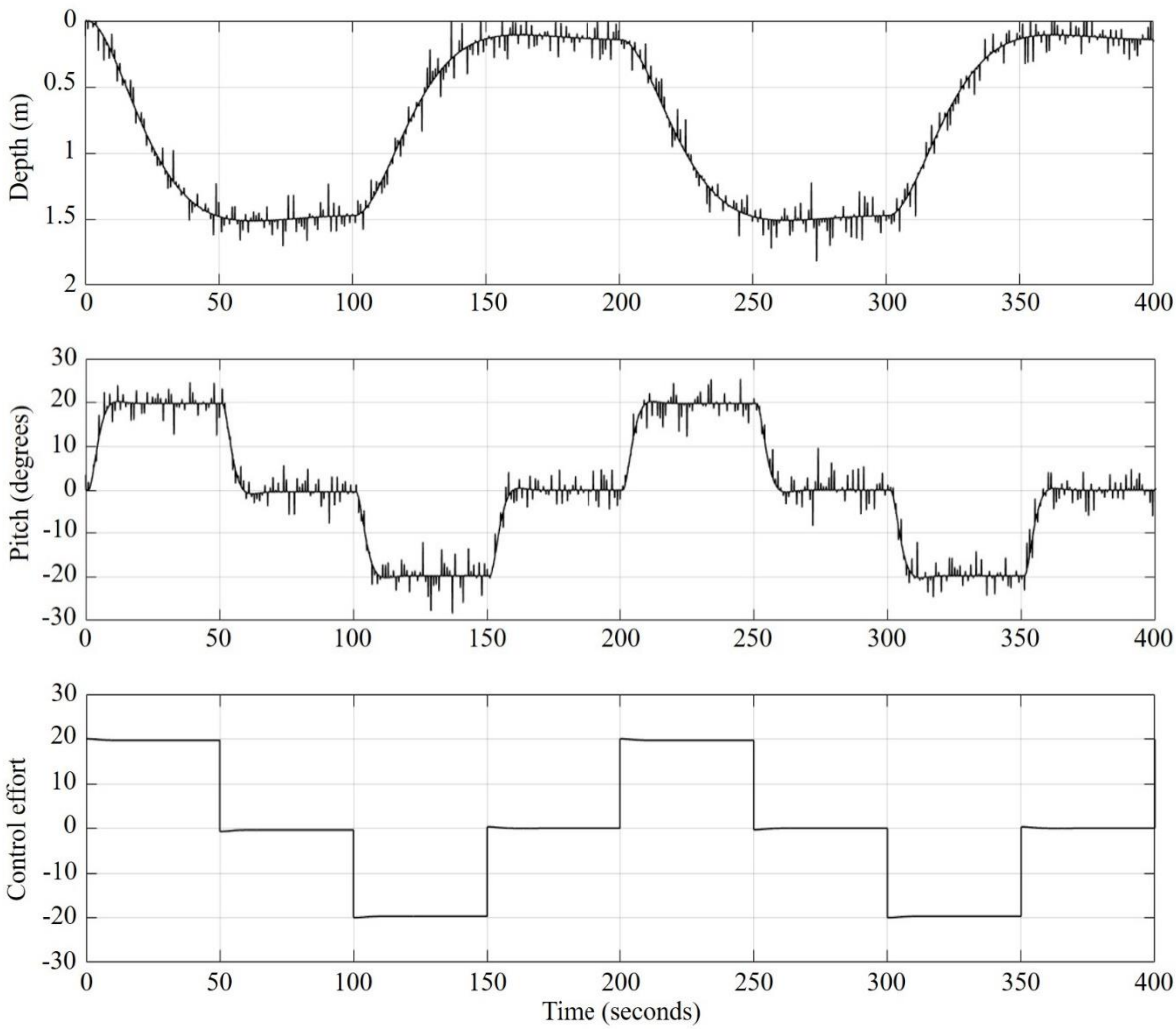

Fig. 9. Results show control performance using LQR controller design

Table 3 summarises the characteristics of the performances. They illustrate the good behaviours. With LQR controller design demonstrates faster response than that of PID controller by 21.84 % and 24.9% for depth and pitch, respectively. Furthermore, LQR control reduces overshoot during transient response by 54.09% and 42.43% for depth and pitch, respectively.

Table 3: Depth and pitch control performance results

Parameter	Depth		Pitch	
	PID	**LQR**	**PID**	**LQR**
%Overshoot	8.56	3.93	2.05	1.18
Settling time (seconds)	115.8	90.5	52.6	39.5
Steady-state error (%)	1.50	0.82	1.22	0.74

5. CONCLUSION

This paper presents the study of modelling and controller designs of the underwater glider. A simplified model has been studied and conducted for preliminary study and experiment. The system identification method provided the estimation of the glider's depth as the output and the control efforts as the input of the system. The best candidate model is chosen to obtain the transfer function. The PID controller with anti-windup compensator is compared with the LQR controller. Both controller designs are demonstrated the good performance. The LQR control presented a better tracking performance with much restrained oscillation and smaller error. However there are several parameters that being neglected in designing the simplified model. Further investigation of a nonlinear system glider will can be carried out.

7. ACKNOWLEDGMENT

This work is supported by the Faculty of Engineering, Burapha University, Thailand (Grant No. 6/2555).

NOMENCLATURE

A_s	Cross section area
C_d	Drag coefficient
C_l	Lift coefficient
$C(\nu)$	Coriolis and centripetal matrix
D_f	Drag
$D(\nu)$	Hydrodynamic damping and lift matrix
$g(\eta)$	Gravity and buoyancy forces and moment matrix
$J(\eta)$	Jacobian matrix
L_f	Lift
m_h	Distribution hull mass
m_p	Fixed point mass
m_b	Variable ballast actuator
m_m	Internal movable mass
M	Inertia and added inertia matrix
M_{DL}	Viscous moment
$[p, q, r]$	Angular velocity vectors about origin in the body-fixed frame
$R_b^n(\eta)$	Linear velocity transformation
$T_b^n(\eta)$	Angular velocity transformation
$[u, v, w]$	Translational motion vectors along the x, y, z –axes
ρ	Fluid density
η	Position vector (x, y, z) and orientation vector (ϕ, θ, ψ)
τ	External force and moment input vector
ν	Linear and angular velocity vector

REFERENCES

[1] Wynn, R.B., Huvenne, V.A.I., Bas, T.P.L., Murton, B.J., Connelly, D.P., Bett, B.J., Ruhl, H.A., Morris, K.J.,Peakall, J., Parsons, D.R., Sumner, E.J., Darby, S.E., Dorrell, R.M. and Hunt, J.E. Autonomous Underwater

Vehicles (AUVs): Their past, present and future contributions to the advancement of marine geoscience, Marine Geology, Vol. 352, 2014, pp. 451-468.
[2] Allotta, B., Caiti, A., Costanzi, R., Fanelli, F., Fenucci, D., Meli, E. and Ridolfi, A. A new AUV navigation system exploiting unscented Kalman filter, Ocean Engineering, Vol. 113, 2016, pp. 121-132.
[3] Wood, S. Autonomous underwater gliders: Underwater vehicles, 2009, IntechOpen, London.
[4] Stommel, H. The slocom mission, Oceanograph, Vol. 2(1), 1989, pp. 22-25.
[5] Webb, D.C., Simonetti, P.J. and Jones, C.P. SLOCUM: an underwater glider propelled by environmental energy, IEEE Journal of Oceanic Engineering, Vol. 26(4), 2001, pp. 447-452.
[6] Sherman, J., Davis, R.E., Owens, W.B. and Valdes, J. The autonomous underwater glider "Spray", IEEE Journal of Oceanic Engineering, Vol. 26(4), 2001, pp. 437-446.
[7] Eriksen, C.C., Osse, T.J., Light, R.D., Wen, T., Lehman, T.W., Sabin, P.L., Ballard, J.W. and Chiodi, A.M. Seaglider: a long-range autonomous underwater vehicle for oceanographic research, IEEE Journal of Oceanic Engineering, Vol. 26(4), 2001, pp. 424-436.
[8] Kawaguchi, K., Ura, T., Tomoda, Y. and Kobayashi, H. Development and sea trials of a shuttle type AUV "ALBAC", paper presented in the International Symposium on Unmanned Untethered Submersible Technology, 1993, Durham, United Kingdom.
[9] Claustre, H., Beguery, L. and Patrice, P. SeaExplorer glider breaks two world records : Multisensor UUV achieves global milestones for endurance, distance, Sea Technology, Vol. 55, 2014, pp. 19-22.
[10] Leonard, N.E. and Graver, J.G. Model-based feedback control of autonomous underwater gliders, IEEE Journal of Oceanic Engineering, Vol. 26(4), 2001, pp. 633-645.
[11] Sliwka, J., Clement, B. and Probst, I. Sea glider guidance around a circle using distance measurements to a drifting acoustic source, IEEE/RSJ International Conference on Intelligent Robots and Systems, 2012, Algarve, Portugal.
[12] Hussain, N.A.A., Chung, T.M., Arshad, M.R., Mohd-Mokhtar, R. and Abdullah, M.Z. Design of an underwater glider platform for shallow-water applications, International Journal of Intelligent Defence Support Systems, Vol. 3(3), 2010, pp. 186-206.
[13] Fossen, T.I. Handbook of marine craft hydrodynamics and motion control, 2011, John Wiley & Sons, New York.
[14] SNAME. Nomenclature for treating the motion of a submerged body through a fluid, Technical and research bulletin, 1952, The Society of Naval Architects and Marine Engineers, New York.
[15] Graver, J.G. Underwater gliders: Dynamics, control and design, Ph.D. thesis, 2005, Princeton University.
[16] Naeem, W., Sutton, R. and Chudley, J. System identification, modelling and control of an autonomous underwater vehicle, IFAC Proceedings, Vol. 36(21), 2003, pp. 19-24.
[17] Aras, M.S.M., Kamarudin, H.N.M., Nor, M.N., Jaadar, A.S.M., Shah, H.N.M., Kassim, A.M., Rashid, M.Z.A. Development and modeling of unmanned underwater remotely operated vehicle using system identification for depth control, Journal of Engineering and Technology, Vol. 4(2), 2013, pp. 1-22.
[18] Mahmoudian, N. and Woolsey, C. Underwater glider motion control, Proceedings of the 47th IEEE Conference on Decision and Control, 2008, Cancun, Mexico.
[19] Asher, B., Steinberg, D.M., Friedman, A.L. and Williams, S.B. Analysis of an autonomous underwater glider, Australasian Conference on Robotics and Automation, 2008, Canberra, Australia.
[20] Noh, M.M., Arshad, M.R. and Mokhtar, R.M. Depth and pitch control of USM underwater glider: Performance comparison PID vs. LQR, Indian Journal of Geo-Marine Sciences, Vol. 40(2), 2011, pp. 200-206.
[21] Tchilian, R.d.S., Rafikova, E., A.Gafurov, S. and Rafikov, M. Optimal control of an underwater glider vehicle, Procedia Engineering, Vol. 176, 2017, pp. 732-740.
[22] Graver, J.G. and Leonard, N.E. Underwater glider dynamics and control, Proceedings of the 12th International Symposium on Unmanned Untethered Submersible Technology, 2001, Durham, United Kingdom.
[23] Yang, H. and Ma, J. Sliding mode tracking control of an autonomous underwater glider, paper presented in the 2010 International Conference on Computer Application and System Modeling, 2010, Taiyuan, China.
[24] Maziyah, M.N., M.R., A., Rosmiwati, M.M., Qudrat, K., Md, Z.Z. and Abdul, K.H. Nonlinear robust integral sliding super-twisting sliding mode control application in autonomous underwater glider, Indian Journal of Geo-Marine Sciences, Vol. 48(7), 2019, pp. 1016-1027.
[25] Mat-Noh, M., Arshad, M.R., Mohd-Mokhtar, R. and Khan, Q. Back-stepping sliding mode control strategy for autonomous underwater glide, The 13th International Conference on Emerging Technologies (ICET), 2017, Islamabad, Pakistan.
[26] Isa, K. and Arshad, M.R. Neural networks control of hybrid-driven underwater glider, Oceans - Yeosu, 2012, Yeosu, South Korea.

[27] Jiang, Q.l., Lei-Han, Wang, X.D., Hua-Yang and Song, D.L. Balance parameters calculation method of underwater glider based on BP neural network, Oceans - Genova, 2015, Genova, Italy.
[28] Leccese, F., Cagnetti, M., Giarnetti, S., Petritoli, E., Luisetto, I., Tuti, S., Durovic-Pejcev, R., Dordevic, T. Tomasevic, A. Bursic, V., Arenella V., Gabriele, P., Pecora, A., Maiolo, L., De Francesco, E., Spagnolo, G.S., Quadarella, R., Bozzi, L. and Formisano C. A simple Takagi-Sugeno fuzzy modelling case study for an underwater glider control system, The 2018 IEEE International Workshop on Metrology for the Sea; Learning to Measure Sea Health Parameters (MetroSea), 2018, Bari, Italy.
[29] Cao, J., Cao, J., Yao, B. and Lian, L. Dynamics and adaptive fuzzy turning control of an underwater glider, Oecans - Genova, 2015, Genova, Italy.
[30] Sang, H., Zhou, Y., Sunb, X. and Yang, S. Heading tracking control with an adaptive hybrid control for under actuated underwater glider, ISA Transactions, Vol. 80, 2018, pp. 544-563.
[31] Abraham, I. and Yi, J. Model predictive control of buoyancy propelled autonomous underwater glider, The 2015 American Control Conference (ACC), 2015, Chicago, United States.
[32] Jantapremjit, P. and Wilson, P.A. Optimal control and guidance for homing and docking tasks using an autonomous underwater vehicle, The IEEE/RSJ International Conference on Intelligent Robots and Systems, 2007, Harbin, China.
[33] Slotine, J.J. and Li, W. Applied nonlinear control, 1991, Prentice Hall, New Jersey.
[34] Goheen, K.R. and Jefferys, E.R. Multivariable self-tuning autopilots for autonomous and remotely operated underwater vehicles, IEEE Journal of Oceanic Engineering, Vol. 13(3), 1990, pp. 144-151.
[35] Nag, A., Patel, S.S. and Akbar, S.A. Fuzzy logic based depth control of an autonomous underwater vehicle, The 2013 International Mutli-Conference on Automation, Computing, Communication, Control and Compressed Sensing (iMac4s), 2013, Kottayam, India.
[36] Fossen, T.I. Guidance and control of ocean vehicles, 1994, Wiley, New Jersey.
[37] Indiveri, G. Modelling and identification of underwater robotic systems, 1998, University of Genova, Italy.
[38] Åström, A.K.J. and Hägglund, T. Advanced PID control, 2006, ISA, United States.
[39] Anderson, B.D.O. and Moore, J.B. Optimal control: Linear quadratic methods, 2007, Dover Publication, United States.